**The North African Journal of Scientific Publishing (NAJSP)**
مجلة شمال إفريقيا للنشر العلمي (NAJSP)
EISSN: 2959-4820
Volume 2, Issue 2, April – June 2024, Page No: 119-129
Website: https://najsp.com/index.php/home/index
**SJIFactor 2023: 3.733** **0.63 :2023 (AIF) معامل التأثير العربي** **ISI 2023: 0.383**

# Adsorption of malachite green from aqueous solutions using carob and eucalyptus twigs: a kinetic and isotherm study

Wafa S. Baej [1*], Abdounasser Albasher Omar [2], Ritaj Fathi Al Touhami [3], Retaj Naserdin Khrwat [4], Sama Abdullah Al Shareef [5]
[1,2,3,4,5] Chemistry Department, Faculty of Science-Gharyan, University of Gharyan, Gharyan, Libya.

*Correspondence: wafa.baej83@gmail.com

| Received: April 30, 2024 | Accepted: June 20, 2024 | Published: June 26, 2024 |
|---|---|---|

**Abstract:**
This study aimed to investigate the adsorption behavior of malachite green (MG) dye on the surfaces of the twigs of carob and eucalyptus plants in aqueous solutions. Carob and eucalyptus twigs were collected from two trees in the city of Gharyan, Libya. Then, the kinetics and adsorption isotherms of the adsorption of MG on both adsorbents were evaluated. The results showed that the surfaces of the twigs of carob and eucalyptus plants adsorbed the dye with almost the same efficiency. The kinetic experiments of the adsorption of MG on both adsorbents were well described by a pseudo-first- order model. And the pseudo-second-order model, the kinetic Elovich model, and the intra-particle diffusion model, where the values of the correlation coefficient ($R^2$) indicated that the adsorption data agree well with the four kinetic models. It has been found that the mechanism of MG adsorption process on carob and eucalyptus follows a chemical adsorption process according to the parameters obtained in the study. The experimental data were analyzed by the Langmuir, Freundlich, Timken, and Dubinin Radushkevich adsorption isotherm models of adsorption. The characteristic parameters for each isotherm and related coefficients of determination were determined. It was found that the adsorption of dye on the surface of carob and eucalyptus is more consistent with the Freundlich model, which proves the non-homogeneity of the surface of the twigs of the two plants. The value of the Tamkin constant $B_t$, which represents the adsorption capacity, agreed closely with the adsorption capacity obtained practically, and the energy of adsorption (E) obtained from D-R isotherm suggests chemical adsorption.

**Keywords:** Malachite green, Carob, Eucalyptus, Adsorption, Kinetics, Adsorption isotherm.

**Cite this article as:** W. S. Baej, A. A. Omar, R. F. Al Touhami, R. N. Khrwat, S. A. Al Shareef, "Adsorption of malachite green from aqueous solutions using carob and eucalyptus twigs: a kinetic and isotherm study," *The North African Journal of Scientific Publishing (NAJSP)*, vol. 2, no. 2, pp. 119–129, April – June 2024.

# إمتزاز صبغتي الميثيل الأخضر والملاكيت الأخضر من المحاليل المائية بواسطة سيقان نباتي الخروب والسرول: دراسة حركية وأيزوثيرم الإمتزاز

وفاء السني بعيج[1*]، عبد الناصر البشيرعمر[2]، رتاج فتحي التهامي[3]، رتاج نصرالدين خرواط[4]، سماء عبد الله الشريف[5]
[1،2،3،4،5] قسم الكيمياء، كلية العلوم، جامعة غريان، غريان، ليبيا

**الملخص**
الهدف من هذه الدراسة هو دراسة سلوك الإمتزاز لصبغة الملاكيت الأخضر (MG) على أسطح سيقان نبات الخروب والسرول في المحاليل المائية، حيث تم جمع سيقان الخروب والسرول المتوفرتين محليا في مدينة غريان، ليبيا. بعد ذلك تم اختيار أفضل توليفة لظروف الامتزاز وذلك للحصول على أعلى كفاءة إمتزاز. وأظهرت النتائج أن أسطح سيقان نباتات الخروب والسرول امتصت الصبغة بنفس الكفاءة تقريبًا، تم إجراء دراسة حركية الامتزازبتطبيق نموذج المرتبة الأولى الوهمية والمرتبة الثانية الوهمية ونموذج الوفيج ونموذج الانتشار داخل الجسيمات، حيث أشارت قيم معامل الارتباط ($R^2$) إلى توافق بيانات الامتزاز بشكل جيد مع النماذج الحركية الأربعة. . وقد وجد أن آلية عملية إمتزاز MG على الخروب والسرول تتبع عملية الامتزاز الكيميائي وفقا للمعايير التي تم الحصول عليها في الدراسة. كذلك تمت دراسة أيزوثرم الإمتزاز بتطبيق نماذج لانجماير وفروندليتش وتيمكين ودوبينين رادوشكيفيتش للامتزاز. وقد وجد أن امتزاز الصبغة على سطح الخروب والكافور أكثر اتساقا مع نموذج فروندليتش الذي يثبت عدم تجانس سطح أغصان النباتين.كما أظهرت الدراسة أن قيمة ثابت تمكين $B_t$ الذي يمثل سعة الامتزاز، تتفق بشكل وثيق مع سعة الامتزاز التي تم الحصول عليها عمليا، وطاقة الامتزاز (E) التي تم الحصول عليها من أيسوثرم D-R تشير إلى الامتزاز الكيميائي.

**الكلمات المفتاحية:** الملاكيت الأخضر، نبات الخروب، السرول، الإمتزاز، حركية الإمتزاز، أيزوثرم الإمتزاز.

## 1. Introduction

Textile, leather, paper, plastics, and cosmetics industries all utilize dyes in production processes, leading to the production of a sizable volume of colored wastewater [1]. Each year, around 700,000 tons of dyestuff and 100,000 commercial dyes are produced, with 10% of the amount of those dyes being released into wastewater from the textile and related industries. When these frequently effluents are dumped into water or land, they cause toxicological and aesthetic harm [2, 3]. Malachite green (MG) is one of the often employed industrial dyes in manufacturing sectors including textile, paper and food processing. Triphenyl methane is the source of this cationic dye. At low pH, MG gains a positive charge (pKa = 10.3) as the auxochrome group is protonated [4]. MG is primarily used to dye wool, silk, acrylic, wood, and paper and leather. Additionally, it is employed in the fish farming business to treat bacterial, fungal, and parasitic illnesses. It has a wide range of uses, but because it is poisonous, it has a severe impact on both aquatic life and human health when it is present in water [5, 6]. It has teratogenic effects on the neurological system and brain, as well as harm to the liver, spleen, kidney, and heart. It also causes lesions to the skin, eyes, lungs, and bones. Generally speaking, the release of dyes into water resources, even in small amounts, is aesthetically displeasing, inhibits light penetration, and alters the gas solubility for photosynthesis and respiration activities [7, 8]. However, physical interaction with several methods, including precipitation [9], flocculation [10], adsorption [11], ion exchange [12], and membrane separation [13], can be used to remove dyes from water. Adsorption is said to be the most straightforward and economical method [11]. At the moment, research is focused on the development of inexpensive adsorbents for removal of chemicals. Natural, agricultural, and industrial by-product wastes can be used as inexpensive adsorbents due to their widespread availability at low or no cost, and due to their effective removal of dyes from aqueous solutions. A number of low-cost materials have been used to remove dyes from aqueous solutions. These include: olive pomace [14, 15], corn cob [16], neem sawdust [17], pulverized teak leaf [5], almond shells [11, 18], Brachychiton Populneus fruit shell [19] rice husks [20]. Also, eucalyptus [21, 22], seeds and bark of carob [23, 24] have been used.

The goal of the current research was to investigate the adsorption behavior of malachite green (MG) on the surfaces of the twigs of carob and eucalyptus plants in aqueous solutions.

## 2. Material and Methods

### 2.1 Chemicals:

The source of the MG was BDH (BDH Chemicals, Poole, UK). Double distilled water was used to prepare all the solutions. A stock solution of malachite green was prepared by dissolving 0.1g of malachite green in 1000 mL of water to obtain a solution of malachite green with a concentration of 100 ppm. The rest of standard solutions were prepared by dilution.

### 2.2 Sampling and preparation for the adsorption process:

A sample was collected from the twigs of the carob plant and the twigs of the eucalyptus plant, from two trees in the city of Gharyan, Libya. After collecting those twigs, they were washed well to remove impurities, and then left to dry for 48 hours. After that, the samples were kept in a plastic bag.

The calibration curve was set using MG solutions at concentrations of 1, 5, 10, 15 and 20 ppm. The absorbance of all standard solutions was measured at 630 nm using a Vis spectrophotometer (6300 Spectrophotometer, Jenway, Staffordshire, UK). The relationship between absorbance and concentration of a standard solution was plotted using Microsoft Excel 2010.

### 2.3 Determination of percentage removal of MG:

A triplicate sample of 1 gram of carob plant twigs and eucalyptus plant twigs was weighed and transferred to clean and dry vials. A volume of 50 mL of MG solution (10 ppm; pH=6) was added to each weight of the twigs of the carob plant and the twigs of the eucalyptus plant. These vials were covered with caps and left at 30° C without shaking for some time. After 5, 10, 20, 30, 40, 50, and 60 minutes, a volume of 4 mL of the green malachite solution was withdrawn and the absorbance was measured using distilled water as a reference solution. After determination of the remained MG concentrations with the aid of the calibration curve, the removal percentage of MG was calculated by equation (1).

$$\text{Removal percentage} = 100\ (C_i - C_{rem})/C_i \qquad (1)$$

Where $C_i$ represents the initial MG concentration and $C_{rem}$ represents the remained MG concentration after each adsorption experiment.

### 2.4 Kinetic Studies:

#### 2.4.1 Pseudo-first order and pseudo-second order:

The adsorption kinetics were studied at a temperature of 30 °C, a concentration of 10 ppm, a pH of 6, and a shaking speed of 50 rpm. Several solutions were prepared with the same concentration of 10 ppm in a volume of 50 mL and placed in vials containing 0.5 g of carob plant twigs or eucalyptus plant twigs.

The solution was shaken and samples were drawn after each 5 min (5 - 60) minutes. Absorbance was measured to determine the amount of remaining and adsorbed MG, and kinetic models were applied to the data. The adsorption capacity of plant twigs at any time, $q_t$, (mg/g) was calculated using equation (2), while the equilibrium adsorption capacity of plant twigs, $q_e$ (mg/g), was calculated using equation (3)

$$q_t = V(C_0 - C_t)/m \qquad (2)$$

$$q_e = V(C_0 - C_e)/m \qquad (3)$$

Where $C_0$ represents the initial MG concentration, $C_t$ represents the remained MG concentration after t time, $C_e$ represents the remained MG concentration after equilibrium time, V represents MG solution volume (L), and m represents the weight of the carob or eucalyptus sample (g).

The obtained data were used to investigate the adsorption kinetics. Two adsorption kinetic models, pseudo-first order stated in equation (4) and pseudo-second-order given in equation (5), were used to achieve this.

$$\mathrm{Log}(qe - qt) = \log(qe) - \frac{K_1 t}{2.303} \qquad (4)$$

$k_1$ is the equilibrium rate constant of pseudo first-order adsorption ($min^{-1}$) and $q_e$ and $q_t$ denote the quantity of dye adsorbed (mg/ g) at equilibrium time and at any time, respectively. If the model fits the experimental data, a linear relationship could be found by plotting log ($q_e$-$q_t$) versus (t), and the constants $k_1$ and estimated $q_e$ could be found from the slope and intercept of the plot [25].

$$\frac{T}{q_t} = \frac{1}{k_2\, q_e^2} + \frac{t}{q_e} \qquad (5)$$

Where $k_2$ (g $mg^{-1}$ $min^{-1}$) is the pseudo-second-order adsorption equilibrium rate constant. If the model fits the experimental data, a linear relationship could be found by plotting $t/q_t$ versus t. The slope and intercept of the plot allow for the determination of the constants $q_e$ and $k_2$, respectively [26].

#### 2.4.2 Elovich Kinetic Model:

Roginsky and Zeldovich proposed an equation known as the Elovich model [2, 27]. It takes into account the chemisorption kinetics and dye molecule diffusion as the rate-controlling step factor. This model

has been successfully applied to systems in which the adsorption surface is heterogeneous. The Elovich kinetic model is expressed by the equation (6) [28].

$$q_t = \left(\frac{1}{\beta}\right) \ln \alpha\beta + \left(\frac{1}{\beta}\right) \ln t \qquad (6)$$

Where $q_t$ is the quantity of adsorbate adsorbed at time t (mg/g), α (mg mol/g min) is the initial adsorption rate and β (g/ mg mol) is the Elovich coefficient related to the extent of surface coverage and activation energy. α and β can be calculated from the intercept and slope of the plot of qt versus (ln t ) respectively .

**2.4.3 Intraparticle Diffusion Kinetic Model:**

Equation 7 describes this model:

$$q_t = k_{id}\, t^{1/2} + C \qquad (7)$$

$k_{id}$ is the scattering constant (mg·g$^{-1}$ min$^{1/2}$), and C is the intercept of a straight line, while $q_t$ is the amount of MG mass adsorbed per mass unit (mg/g) at time t. The mass absorbed ($q_t$) vs. $t^{1/2}$ graph was used to fit the data into a linear regression. The intra-particle diffusion constants ($k_{id}$) were derived from the slope, and the C values were calculated from interceptions with the vertical axis [2, 23].

**2.5 Adsorption Isotherms:**

To obtain the adsorption isotherm, different concentrations of MG solutions (2, 3, 5, 7.5, 10, 12.5, 15, 20) ppm of MG were prepared, and 50 ml of solutions of these concentrations were added to vials containing a fixed weight of carob and eucalyptus twigs (0.5 g), at a pH of 6. Then, the vials were placed in an orbital shaker at a speed of 50 rpm and a temperature of 30° C.

All solutions were left for 80 minutes, and then the absorbance of each solution was recorded. Based on the absorbance values, the concentration of the remained and the adsorbed MG was calculated, and the isotherm models were applied to the data.

**2.5.1 Langmuir isotherm**

This model assumes that there will be equal amounts of surface heat absorption and monolayer formation. The linearization form is shown in equation (8).

$$\frac{C_e}{q_e} = \left(\frac{1}{q_{max}}\right) C_e + \frac{1}{K_L\, q_{max}} \qquad (8)$$

Where $K_L$ is a constant referring to the energy of adsorption (L/mg), and qmax is the maximum Langmuir constant associated with adsorption capacity (mg/g). By calculating the slope of the linear plot of Ce/qe vs. $C_e$, it is possible to determine $q_{max}$ and $K_L$ from Eq. (8).

**2.5.2 Freundlich isotherm**

The depiction of the surface energy is accomplished using the equation given by equation (9)

$$\log q_e = \log K_f + \frac{1}{n} \log C_e \qquad (9)$$

$K_f$ (mg/g) is a constant relating to the sorbent's ability for adsorption, and n is the adsorption intensity. Based on the value of n, poor, moderate, and good characteristics of adsorption identified for n = 1, n = 1-2, and n = 2-10, respectively [31].

**2.5.3 Temkin isotherm**

The Temkin isotherm model's linearized form is expressed as in equation (10)

$$q_e = B_t \ln K_t + B_t \ln C_e \qquad (10)$$

$K_t$ is the equilibrium binding constant (L/g) corresponding to the maximum binding energy, $B_t$ = (RT/b) is Temkin constant (J/kJ), b is the heat of adsorption (kJ/mol), R is the universal gas constant (8.314 J/mol K), and T is the absolute temperature (K) [32].

**2.5.4 Dubinin-Radushkevich Isotherms**

The linear form of the Dubinin-Radushkevich (D-R) adsorption isotherm was used to fit the data. This model is typically used (equation (11)) to describe the adsorption mechanism with a Gaussian energy distribution on a heterogeneous surface.

$$\ln q_e = \ln q_s - \beta\, \varepsilon^2 \qquad (11)$$

Where $q_e$ is the quantity of adsorbate in the adsorbent at equilibrium (mg g$^{-1}$), $q_s$ is the theoretical isotherm saturation capacity (mg g$^{-1}$), β (mol$^2$ /J$^2$ ) is the activity coefficient helpful in determining the

mean sorption energy E (kJ/mol) and Ɛ is the Polanyi potential. Ɛ and E are expressed by equations (12) and (13) respectively

$$E = \frac{1}{\sqrt{2\beta}} \qquad (12)$$

$$\varepsilon = RT \ln\left(1 + \frac{1}{C_e}\right) \qquad (13)$$

Where R is the gas constant (8.314 J/mol K) and T is the temperature (K). And $q_s$ and β can respectively be calculated from the intercept and the slope of the plot of ln qe vs $\varepsilon^2$ [5, 33].

## 3. Results and Discussion:

In each adsorption experiment, the remained MG concentration was calculated using the regression equation expressed in equation (14), which was obtained by using standard MG solutions (2–20 ppm) at pH =6. This equation's coefficient of determination ($R^2$) was 0.9924, indicating high linearity. As a result, this equation was statistically valid for calculating the remaining MG concentration.

$$A = 0.1558\ C + 0.1308 \qquad (14)$$

Where A is the absorbance of each MG solution, and C is MG concentration in ppm.

### 3.1 Efficiency of carob and Eucalyptus tree twigs in removing MG from aqueous solutions:

As shown in Figure (1), both adsorbents adsorbed MG from aqueous solutions with comparable efficiency. It was also noted that MG adsorption increased with time. After 5 minutes, the percentage of MG adsorption on the twigs of the carob and eucalyptus trees was 23.7% and 22.8%, respectively, and the percentage of adsorption more than doubled after 60 minutes, reaching 50.33% on the carob twigs and 49.05% on the eucalyptus twigs.

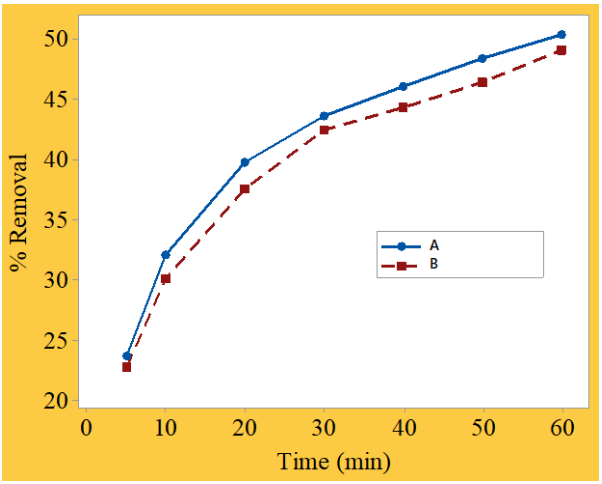


**Figure (1):** Percentage of MG adsorption on carob twigs (A) and eucalyptus twigs (B).

### 3.2 Adsorption kinetics:

The equilibrium time for MG adsorption on carob twigs was 70 minutes and 60 minutes on eucalyptus twigs.

The results obtained from the kinetic studies were used in the application of pseudo first-order and pseudo second-order kinetic models for the adsorption of MG on the surface of carob and eucalyptus twigs (Figure 2 (a, b, c and d)), and the kinetic parameters obtained are given in Table 1.

As sown in Table 1, the pseudo first-order and pseudo second-order kinetics were both good in fitting the experimental data for both adsorbents. However, the value of $R^2$ for the pseudo second-order model was higher for both adsorbents, indicating that the adsorption process of the dye on the surface of the carob and eucalyptus plants both follows the pseudo second-order kinetic model.

The maximum adsorption capacity ($q_{max}$) was calculated and the theoretical values calculated using this model at equilibrium were close to those experimentally determined values. We could therefore adopt

the hypothesis of chemisorption resulting from an electron exchange between the dye cations and the functional groups of the adsorbents [34].

Several previous studies on the adsorption of MG on (Walnut Shells, activated carbon derived from oil palm empty fruit bunches, modified and unmodified local agriculture waste) [35-37] also showed that this phenomenon obeyed the pseudo-second-order. Adsorption rate constant ($K_2$) for carob were (0.0279 g.mg$^{-1}$.min$^{-1}$) smaller than adsorption rate constant for eucalyptus (0.0882 g.mg$^{-1}$.min$^{-1}$), reflecting that the adsorption of MG on the eucalyptus twigs occurs faster than on the surface of the carob twigs.

**Table (1):** coefficient of determination ($R^2$) and constants of kinetic models for the adsorption of MG onto carob and eucalyptus.

| Constant | Carob | Eucalyptus |
|---|---|---|
| $q_e$ experimental (mg/g) | 0.5874 | 0.5338 |
| **Pseudo first order** | | |
| $q_e$ calculated (mg/g) | 0.7166 | 0.5418 |
| $K_1$ ( min$^{-1}$) | 0.0446 | 0.0533 |
| $R^2$ | 0.955 | 0.972 |
| **Pseudo second order** | | |
| $q_e$ calculated (mg/g) | 0.8953 | 0.6596 |
| $k_2$ (g·mg$^{-1}$ min$^{-1}$) | 0.0279 | 0.0882 |
| $R^2$ | 0.996 | 0.991 |
| **Elovich** | | |
| α (mg/g min) | 0.051705 | 0.08303 |
| β (g/mg) | 5.374 | 6.854 |
| $R^2$ | 0.981 | 0.986 |
| **Intra particle diffusion** | | 0.04162 |
| C (mg /g) | -0.06114 | 0.06543 |
| $K_{id}$ (mg/g min$^{1/2}$) | 0.07879 | 0.994 |
| $R^2$ | 0.996 | |

The Elovich model was tested for the adsorption of MG on both adsorbents by plotting $q_t$ against ln (t) as shown in Figure 2 (e,f); the model constants (β and α), as well as $R^2$ are presented in Table 1.

The values of $R^2$ for the adsorption process of MG on carob and eucalyptus twigs were 0.981 and 0.986 respectively. These values of $R^2$ indicated that the adsorption data fitted well to the Elovich kinetic model. Values of α were small, while those for β were large for both adsorbents and β values were greater than α for the two adsorbent materials, thus desorption is greater than adsorption at a temperature of 30 °C. as shown in table 1 [27].

For the intraparticle diffusion mode, Figure 2 (g, h) depicts the plots of $q_t$ against $t^{1/2}$ values for the adsorption of MG on the surface on both adsorbents. The figure shows the strong positive linear relationship between $q_t$ and $t^{1/2}$ values, with close $R^2$ for the adsorption on the surfaces of both adsorbents; 0.996 for carob and 0.994 for eucalyptus (Table 1). This implied that the adsorption process followed the intraparticle diffusion model. However, none of the plots passed through the origin. If the linear portion of the intraparticle diffusion kinetic plot does not pass through the origin, then some extent of boundary layer control is involved, and that intraparticle diffusion is not the single rate controlling step [38]. The $K_{id}$ value for the adsorption of MG on carob twigs was greater than the $K_{id}$ value for the adsorption of MG on the eucalyptus twigs. Therefore, the speed of diffusion of dye molecules on carob twigs is greater than the speed of diffusion on eucalyptus twigs. The values of $k_{id}$ and C are shown in Table 1.

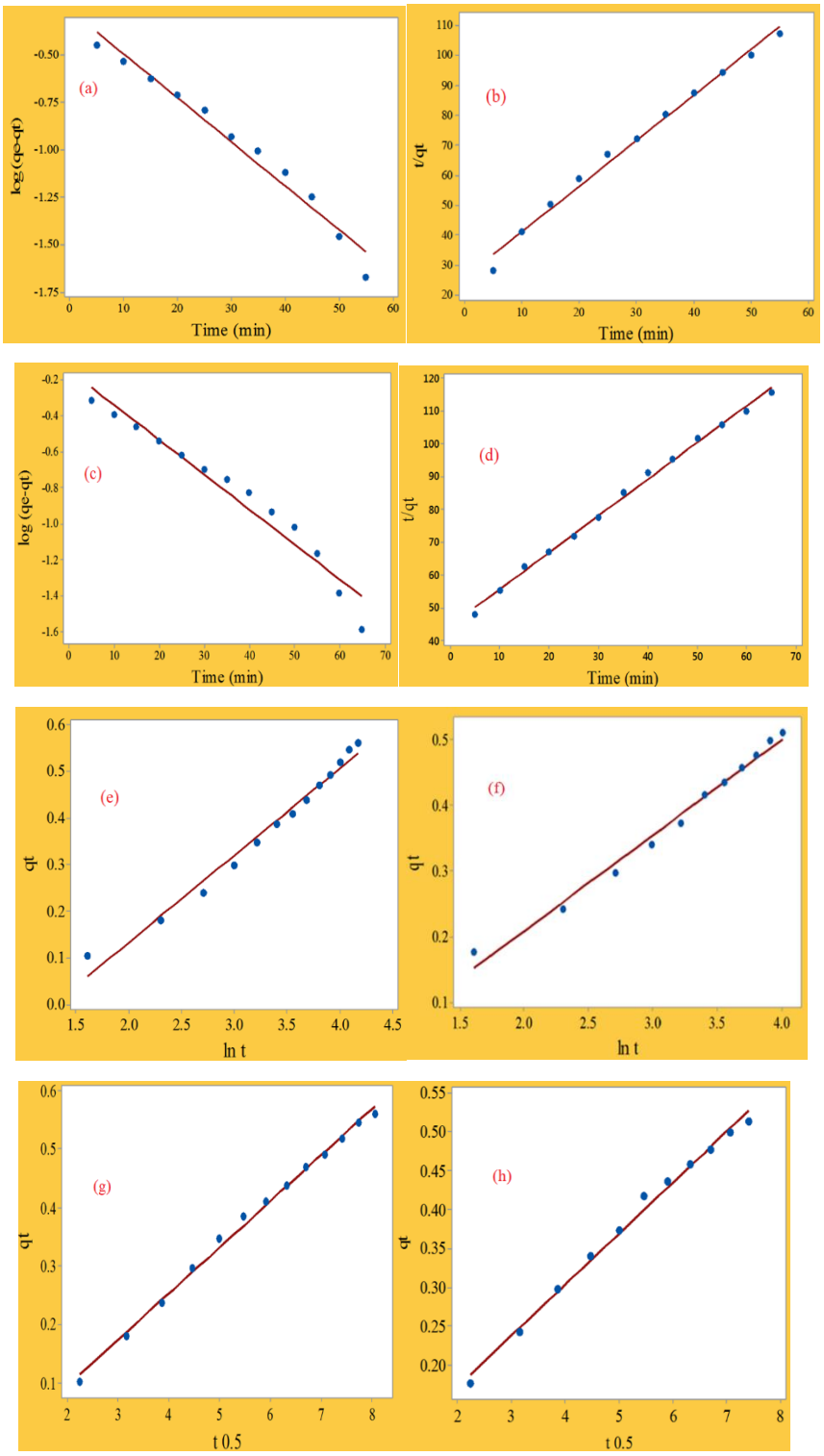


**Figure 2**: Pseudo first-order (a) and pseudo second order (b) for MG adsorption onto Eucalyptus twigs. Pseudo first-order (c) and pseudo second order (d) for MG adsorption onto carob twigs, The Elovich model plots for uptake of MG onto carob (e) and Eucalyptus (f) twigs, and Intraparticle diffusion model plots for uptake of MG onto carob (g) and Eucalyptus (h) twigs.

### 3.3 Adsorption isotherm:

Adsorption isotherms (Langmuir, Freundlich, Temkin, and Dubinin-Radushkevich (D-R) models) were used in the present study. The results are presented in Table (2) which shows the modelled isotherms.

As shown in table (2), the values of the correlation coefficient ($R^2$) resulting from applying the Langmuir model were small, thus the adsorption of the dye on the surface of carob and eucalyptus

twigs does not agree with the Langmuir model. Therefore, the constants related to the Langmuir model were not calculated.

**Table 2:** Parameters for plotting Langmuir, Freundlich, Temkin and Dubinin-Radushkevich adsorption isotherms of MG onto carob and eucalyptus twigs.

| Isotherms | constants | Carob | Eucalyptus |
|---|---|---|---|
| Lagmuir | $R^2$ | 0.626 | 0.439 |
| Freundlich | $k_f$ (mg/g)<br>$(L/mg)^{1/n}$<br>N<br>$R^2$ | 0.0282<br>0.7267<br>0.942 | 0.0276<br>0.7874<br>0.936 |
| Temkin | $B_t$ (J/mol<br>$K_t$ (L/g)<br>$R^2$ | 0.6721<br>0.303814<br>0.784 | 0.5421<br>0.298055<br>0.81 |
| D-R | $q_o$ (mg/g)<br>β ($mol^2\ k_J{}^{-2}$)<br>E $(Jmol^{-1})^2$<br>$R^2$ | 0.89048<br>0.000005<br>316.228<br>0.797 | 0.73558<br>0.000005<br>316.228<br>0.772 |

Also, for the adsorption of MG on carob and eucalyptus twigs, the results presented in Table (2) show that Freundlich isotherm gave a good fit to the experimental equilibrium adsorption data than that of Langmuir, Dubinin-Radushkevich, and Temkin isotherm models according to the values of $R^2$. Moreover, values of n, which give an idea about the adsorption intensity, were calculated for carob and eucalyptus; the n values showed that the adsorption was chemisorption and a multilayer adsorption on a heterogeneous surface [34].

Values of n were less than 1 for MG adsorption on carob twigs and eucalyptus twigs, 0.7267 and 0.7874 respectively, therefore the values of 1/n are greater than 1 implying that the adsorbent surface is not homogeneous. The reason is due to the difference in active site adsorption and the difference in active site energies. The $K_f$ values, which give information about the adsorption capacity, were similar for the adsorption of the dye on the surfaces of carob and eucalyptus. Therefore, the adsorption capacity of the surfaces of carob and eucalyptus are similar [39-41]. This result agrees with many previous studies when (eucalyptus sawdust, eucalyptus Camdulensis, Biochar and Carob (Ceratonia siliqua)) have been used as adsorbent surfaces for some dyes, as the experimental data fit the Freundlich model [22,24,42].

When the Tamkin model was applied, the value of the correlation coefficient ($R^2$) for the adsorption of MG on the surface of eucalyptus twigs was 0.810, which was greater than the value of $R^2$ (0.784) for the adsorption of MG on the surface of carob twigs. Therefore, the adsorption of the dye on the eucalyptus twigs surface fits the Tamkin model better than its adsorption on the surface of the carob twigs. The values of the constant $B_t$, which is related to the adsorption capacity, agree with the values of the adsorption capacity obtained practically, Also, the value of the constant $B_t$ for MG adsorption on the surface of carob twigs was slightly higher than on the surface of eucalyptus twigs. Thus, the surface of the carob adsorbed MG a little more than the eucalyptus. Also, the values of $K_t$, which represents the energy of interaction between the dye and the surface of the adsorbent material, were very close for the adsorption of the dye on the surface of the carob and eucalyptus twigs.

The adsorption results were analysed according to the linear D-R isotherm, which is considered more comprehensive than the Langmuir and Freundlich method on the heterogeneous surface, as the energy equation (Eq (12)) gives an idea of the adsorption mechanism [43]. The energy values resulting from the adsorption of the dye on the surface of the carob and eucalyptus were equal (316.228 kj/mol). This value is considered large and indicates that the adsorption mechanism depends on ion exchange followed by complexation with chemical adsorption [44,45]. Furthermore, the $R^2$ value for adsorption of MG on the surface of carob twigs (0.797) is slightly higher than the $R^2$ value for adsorption of MG on the surface of eucalyptus twigs (0.772). Therefore, the adsorption of the dye on the carob surface fits the DR model slightly better than its adsorption on the surface of the eucalyptus.

Briefly, by comparison, the order of the isotherm best fits experimental data for carob twigs is: Freundlich > Dubinin-Radushkevich > Timken > Langmuir
And the order of the isotherm best fits experimental data for eucalyptus twigs is: Freundlich > Timken> Dubinin-Radushkevich > Langmuir

**4. Conclusion:**

This study showed the possibility of using the twigs of the carob and ecalyptus plants to adsorb malachite green dye from aqueous solutions, especially at low concentrations. This indicates the possibility of using the twigs of the carob plant and the ecalyptus plant to reduce the concentrations of many dyes in aqueous solutions. The results showed that the twigs of the carob and ecalyptus plants absorbed the MG dye with almost the same efficiency, as the equilibrium time for the MG dye on the surface of the eucalyptus twigs was 60 minutes and on the surface of the carob twigs was 70 minutes.
Comparison of kinetic models applied to MG adsorption on carob and eucalyptus twigs to pseudo first- and second-order models, Elovich models, and intraparticle diffusion kinetics was evaluated.
The experimental data agree well with the four models and were in the following order on the surface of carob twigs:
Pseudo second order = Intra particle diffusion> Elovich> Pseudo first order.
and were in the following order on the surface of eucalyptus twigs:
Intra particle diffusion>Pseudo second order>Elovich >first- order model.
The results for adsorption isotherms according to the linear equations of Langmuir, Freundlich, Tamkin, and D-R revealed that the dye adsorption process was more consistent with the Freundlich model, which indicates that adsorption occurs in several layers on the surface of the twigs of the two plants.

**References:**

[1] M. Rafatullah, O. Sulaiman, R. Hashim, and A. Ahmad, “Adsorption of methylene blue on low-cost adsorbents,” a review. Journal of hazardous materials, vol.177, pp. 70-80, May. 2010.
[2] Y. M. Vargas-Rodriguez, et al., “Adsorption studies of aqueous solutions of methyl green for halloysite nanotubes: Kinetics, isotherms, and thermodynamic parameters,” Amer. J. Nanom, vol.9, pp.1-11, 2021.
[3] Y Kerzabi, A. Benomara, and S. Merghache, “Removal of Methyl violet 2B dye from aqueous solution by adsorption onto raw and modified carobs (Ceratonia siliqua L.),” Glob. Nest J, vol.24, pp. 706-719, 2022.
[4] N. B. Swan, and M. A. A. Zaini, “Adsorption of malachite green and congo red dyes from water: recent progress and future outlook,” ECOL CHEM ENG S,vol. 26,no. 1,pp. 119-132, 2019.
[5] E. O. Oyelude, J. A. Awudza, and S. K. Twumasi, “Removal of malachite green from aqueous solution using pulverized teak leaf litter: equilibrium, kinetic and thermodynamic studies,” Chemistry Central Journal, vol.12,no.1,pp. 1-10, 2018.
[6] M. E. Yonar, and S. M. Yonar, “Changes in selected immunological parameters and antioxidant status of rainbow trout exposed to malachite green (Oncorhynchus mykiss, Walbaum, 1792),” Pesticide Biochemistry and Physiology, vol. 97, no.1, pp. 19-23, 2010.
[7] D. Wang, L. Liu, X. Jiang, J. Yu, and X. Chen, “Adsorption and removal of malachite green from aqueous solution using magnetic β-cyclodextrin-graphene oxide nanocomposites as adsorbents,” Colloids and Surfaces A: Physicochemical and Engineering Aspects, vol. 466, pp. 166-173, Feb. 2015.
[8] A. S. Sartape, A. M. Mandhare, , V. V. Raut, P. D., M. A. Anuse, and S. S. Kolekar, “Removal of malachite green dye from aqueous solution with adsorption technique using Limonia acidissima (wood apple) shell as low cost adsorbent,” Arabian Journal of Chemistry, vol. 10, pp. S3229-S3238, May. 2017.
[9] S. Wang, and E. Ariyanto, “Competitive adsorption of malachite green and Pb ions on natural zeolite,” Journal of Colloid and Interface Science,vol. 314, no. 1, pp. 25-31, Oct. 2007.
[10] Y. Al-Ani, and Y. Li, “Degradation of CI Reactive Blue 19 using combined iron scrap process and coagulation/flocculation by a novel Al (OH) 3–polyacrylamide hybrid polymer,” Journal of the Taiwan institute of chemical engineers, vol. 43, no.6, pp. 942-947, Nov. 2012.
[11] M. K. Tanaydin, and A. Goksu, “Optimization of the adsorption of methyl green dye on almond shells using central composite design,” Desalination Water Treat, vol. 227, pp. 425-439, Jul. 2021.
[12] S. Stopić, B. Friedrich, and A. Widigdo, “Electrolytic recovery of copper from highly contaminated wastewaters,” Metalurgija, vol. 13,p. 27, 2007.

[13] Y. Zhang, C. Causserand, P. Aimar, and J. P. Cravedi, “Removal of bisphenol A by a nanofiltration membrane in view of drinking water production,” Water research, vol.40, no.20, pp. 3793-3799, 2006.
[14] A. A. Omar, M. M. Saed, M. M. Abdalkarim, H. A. Iedeelah, and W. Beaj, “Olive pomace as an abundant, low-cost adsorbent for nitrate removal from aqueous solution,” MAYFEB Journal of Environmental Science,vol. 1, 2016.
[15] ] W. S. Beaj, A. A. Omar, N. A. Ahmad, H. Almahdi, S. M. A. Alhinsheeri, and M. F. Sheemah, “Adsorption of methyl orange from aqueous solutions using olive pomace: Akinetic and isotherm study,” In The 3rd Annual Conference on Theories and Applications of Basic and Biosciences, Misurata, Libya, pp. 23-33, 2019.
[16] S. N. A. S. Ismail, W. A. Rahman, N. A. A. , Rahim, N. D. Masdar, and M. L. Kamal, “Adsorption of malachite green dye from aqueous solution using corn cob,” In AIP Conference Proceedings,vol. 2031, no. 1, pp.1-5 , Nov. 2018.
[17] S. D. Khattri, and M. K. Singh, “Removal of malachite green from dye wastewater using neem sawdust by adsorption,” Journal of hazardous materials, vol. 167, no.1-3, pp. 1089-1094, Feb. 2009.
[18] D. Ozdes, A. Gundogdu, C. Duran, and H. B. Senturk, “Evaluation of adsorption characteristics of malachite green onto almond shell (Prunus dulcis),” Separation Science and Technology, vol. 45, no.14, pp. 2076-2085, May. 2010.
[19] K. Rida, K. Chaibeddra, and K. Cheraitia, “Adsorption of cationic dye methyl green from aqueous solution onto activated carbon prepared from brachychitonpopulneus fruit shell,” ndian Journal of Chemical Technology, vol. 27, pp. 51-59, Jan. 2020.
[20] ] V. Muinde, J. M. Onyari, B. M. Wamalwa, and J. Wabomba, “Adsorption of malachite green from aqueous solutions onto rice husks: kinetic and equilibrium studies,” vol.8, no. 3, pp. 215-230, Mar. 2017.
[21] L. D. R. Darcie, B. V. Jacon, G. S. Silva Andrade, A. M. Siqueira Oliveira, M. S. Lopes, and T. R. Giraldi, “Eucalyptus sawdust as an alternative adsorbent for rhodamine B dye removal,” DESALINATION AND WATE TREATMENT, vol. 229, pp. 430-440, Jul. 2021.
[22] M. T. Amin, A. A. Alazba, and M. Shafiq, “Successful application of eucalyptus camdulensis biochar in the batch adsorption of crystal violet and methylene blue dyes from aqueous solution,” *Sustainability*,vol. 13, no.7, p. 3600, Mar. 2021.
[23] Y. Kerzabi, A. Benomara, and S. Merghache, “Removal of Methyl violet 2B dye from aqueous solution by adsorption onto raw and modified carobs (Ceratonia siliqua L.),” Glob. Nest J, vol. 24, pp. 1-13, Nov. 2022.
[24] F. Güzel, H. Sayğılı, G. A. Sayğılı, and F. Koyuncu, “New low-cost nanoporous carbonaceous adsorbent developed from carob (Ceratonia siliqua) processing industry waste for the adsorption of anionic textile dye: Characterization, equilibrium and kinetic modeling,” Journal of Molecular Liquids, vol. 206, pp. 244-255, Jun. 2015.
[25] H. Yuh-Shan, “Citation review of Lagergren kinetic rate equation on adsorption reactions,”Scientometrics, vol. 59, no.1, pp.171-177, Jan. 2004.
[26] ] E.L. Cochrane , S. Lu , S.W. Gibb , and I. Villaescusa, “A comparison of low-cost biosorbents and commercial sorbents for the removal of copper from aqueous media,” Journal of hazardous materials, vol. 137, no. 1, pp. 198-206, Sep. 2006.
[27] K. I. Al-Niemi, “Application of kinetic model of adsorption for Elovich and the intraparticles diffusion, the Sticking probability (S*), Tempkin isotherm on some different aromatic and aliphatic acids,” Journal of Education and Science, vol. 28, no. 1, pp. 246-272, 2019.
[28] C. Aharoni, and M. Ungarish, “Kinetics of activated chemisorption. Part 1.—The non-elovichian part of the isotherm”. Journal of the Chemical Society, Faraday Transactions 1: Physical Chemistry in Condensed Phases, vol. 72, pp. 400-408.
[29] A. Belgacem, I. Ould Brahim ,M. Belmedani, and H. Hadoun, “Removal of methyl green dye from aqueous solutions using activated carbon derived from cryogenic crushed waste tires,” Iranian Journal of Chemistry and Chemical Engineering, vol. 41, no. 1, pp. 207-219, 2022.
[30] S. M. Alardhi, J. M. Alrubaye, and T. M. Albayati, “Adsorption of Methyl Green dye onto MCM-41: equilibrium, kinetics and thermodynamic studies,” Desalination and Water Treatment, vol. 179, pp. 323-331,Mar. 2020.
[31] A. Mittal, “Adsorption kinetics of removal of a toxic dye, Malachite Green, from wastewater by using hen feathers,”Journal of hazardous materials,vol. 133, no(1-3), pp.196-202, May. 2006.
[32] Y. Kim, C. Kim, I. Choi, S. Rengaraj, and J. Yi, “Arsenic removal using mesoporous alumina prepared via a templating method,” Environmental science & technology, vol. 38, no. 3, pp. 924-931, 2004.
[33] N. A. Udoka, and C. Enenebeaku, “Proficiency of Graphene Oxide in Adsorption of Zn (II) Ions from Aqueous Solution,” Physical Chemistry Research, vol.7,no. 2, pp. 295-307, Mar. 2019.

[34] Y. Satlaoui, et al. “Removal properties, mechanisms, and performance of methyl green from aqueous solution using raw and purified sejnane clay type,” Journal of Chemistry, Aug. 2019.
[35] S. Merrad, M. Abbas, M. Trare, . “Adsorption of Malachite Green onto Walnut Shells: Kinetics, Thermodynamic, and Regeneration of the Adsorbent by Chemical Process,” *Fibers and Polymers*. vol. 24, no. 3, pp. 1067-1081, Mar. 2023.
[36] T. Somsiripan and C. Sangwechien,. “Enhancement of adsorption capacity of Methylene blue, Malachite green, and Rhodamine B onto KOH activated carbon derived from oil palm empty fruit bunches,” *Arabian Journal of Chemistry*, vol. 16. no.12, pp. 105270, Dec. 2023.
[37] M .S. Bashanaini, M. H. Al-Douh, and H.S. AL-Ameri, H. Saeed, “Removal of malachite green dye from aqueous solution by adsorption using modified and unmodified local agriculture waste,” *Science Journal of Analytical Chemistry*, vol. 7. no.2, pp. 42-56, Jun. 2019.
[38] S. M. Yakout and E. Elsherif , “Batch kinetics, isotherm and thermodynamic studies of adsorption of strontium from aqueous solutions onto low cost rice-straw based carbons,” *Carbon – Sci. Tech*, vol.1, pp. 144 -153, 2010.
[39] F.Haghseresht, G. Q. LU, “Adsorption characteristics of phenolic compounds onto coal-reject-derived adsorbents,” *Energy & Fuels*, vol.12, no. 6, pp. 1100-1107, Sep. 1998.
[40] A. F. Dawood, A. A. AL- Taie, and M. I. A.Mubarak, “Study Eosin Dye Adsorption on the Surface Wa ste of Molasses Dates Production,” *Diyala Journal For Pure Science*, vol. 13, no.1, Jan. 2017.
[41] V. S. Mane, and P. V. Babu, “Kinetic and equilibrium studies on the removal of Congo red from aqueous solution using Eucalyptus wood (Eucalyptus globulus) saw dust,” *Journal of the Taiwan Institute of Chemical Engineers*, vol. 44, no.1, pp. 81-88, Jan. 2013.
[42] M. A. AL-Ghouti, D.A. DA'ANA, “Guidelines for the use and interpretation of adsorption isotherm models: A review,” *Journal of hazardous materials*, vol.393, pp. 122383, Jul. 2020.
[43] M.M.Dubinin, and L.V.Radush kevich, “Equation of the characteristic curve of activated charcoal,”Proc.Acad.Sci.Phys. Chem.USSR55, pp.331–333,1947.
[44] I. Mobasherpour, E.Salahi, and M. Pazouki, “Removal of divalent cadmium cations by means of synthetic nano crystallite hydroxyapatite,” *Desalination*, vol. 266. no.1-3, pp. 142-148, Jan. 2011.
[45] A. A. ALshuiref, et al., “Equilibrium, Kinetic, and Thermodynamic Study of The Adsorption of Cu (II) From Aqueous Solution Using Activated Carbon Derived From Acacia,” JOURNAL OF MARINE SCIENCES & ENVIRONMENT TECHNOLOGIES, vol. 6, no. 2, pp. 29-48, 2020